Transition to space-time chaos in a nonlinear optical system with two-dimensional feedback

P. L. Ramazza,[1] S. Residori,[1] E. Pamapaloni,[1] and A. V. Larichev[2]
[1]*Istituto Nazionale di Ottica, Largo Enrico Fermi 6, 50125 Firenze, Italy*
[2]*International Laser Center, Moscow State University, 199899 Moscow, Russia*
(Received 20 June 1995)

By varying an intensive parameter in a nonlinear optical system with two-dimensional feedback the wave front displays a transition from a uniform to a patterned state, and eventually to space-time chaos. A nonlocal interaction, introduced by means of a feedback rotation, is the source of the observed phenomena. The observed space-time chaotic behavior is characterized by a rapid decay of correlation. We study the possibility that the system eventually evolves from space-time chaos to a turbulent regime.

PACS number(s): 42.65.Sf, 05.45.+b

I. INTRODUCTION

The issue of pattern formation and competition and, more generally, of complex behavior in extended systems, has recently attracted the attention of researchers working in many areas of physics [1] and of other sciences, such as chemistry [1,2] and biology [2]. In this context nonlinear optics has attained a relevant role [3], due to its peculiar attitude in coupling together different fundamental physical effects as diffraction, diffusion, and nonlinear interaction between electromagnetic fields and matter, thus allowing the study of models and experiments that can often be considered as metaphors for broader classes of phenomena.

Ordered patterns with symmetries induced by the transverse boundaries of the experimental system have been known in linear optics for a long time. Some examples are the modes of an optical resonator [4] or even diffraction fringes from an aperture. However, only recently have detailed experiments been reported on the interaction among these structures in the presence of a nonlinear coupling [5]. A satisfactory description of this nonlinearity has been accomplished either via the application of normal form equations [6] or by using numerical simulations [7].

Another kind of regular pattern, whose symmetry can be either intrinsic of the nonlinear media used, or dependent on the transverse boundary, arises in the wave front of a light beam due to the coupling of optical nonlinearities either with nonlocal interactions [8] or diffraction [9]. In the case of a two-dimensional (2D) nonlocal feedback, patterns consist of multipetal structures and rotating waves [10]. In the diffractive case, patterns characterized by an hexagonal symmetry have been theoretically predicted [9] and experimentally observed [11]. The effect of the transverse boundary was also investigated both theoretically [12] and experimentally [13]. The combination of diffraction and nonlocality, introduced as a rotation of the field in the feedback loop, gives rise to a new class of spatial patterns called ''Akhseals'' [14], in memory of the late Moscow physicist Akhmanov. For particular values of the feedback rotation angle, types of competition similar to ones existing in hydrodynamical systems, namely hexagon-roll transitions, have been shown to exist [15], and also quasi-crystal-like structures have been observed [16].

Several examples of transitions from ordered patterns to more complex or even space-time chaotic situations have been reported in photorefractive oscillators [5,17], in lasers [18], and in liquid-crystal-based devices [19]. The transitions arise when increasing the Fresnel number; that is, the optical aperture of the experimental systems.

Space-time chaos in a spatially extended system can be defined as a regime in which the spatial correlation length of the signal is much shorter than the system size, and the temporal dynamics inside any spatial correlation domain is chaotic [20]. Typical indicators for detecting the presence of space-time chaos regimes are therefore the spatial correlation length of the signal (or, equivalently, its spatial power spectrum) and the local temporal correlation length. Indeed, though several indicators preferable to time correlation length exist in order to detect temporal chaos (e.g., correlation dimension, Lyapunov spectra), a reliable evaluation of all these quantities is possible only in the case of low-dimensional dynamical systems. This is clearly not the case when the signal is formed by a collection of many spatially uncorrelated domains.

The study of optical high-dimensional systems has revealed the presence of phase singularities in the optical wave fronts, whose role is to limit the correlation length of the patterns [17]. Furthermore, in systems exhibiting an intrinsic cutoff length due to diffusion, it has been shown that the boundary influence on pattern formation ceases to be relevant in the high Fresnel number limit [21].

The above reported order-disorder transitions occur for increasing values of an extensive parameter, namely, the Fresnel number. This in fact puts strong limitations on drawing a comparison with other branches of physics, where transitions are mainly driven by an intensive parameter. Though numerical evidence exists that nonlinear optical systems could also exhibit order-disorder transitions versus an intensive parameter (pump rate in lasers [22], intensity in Kerr-like systems [9]) from the experimental side, the only examples of an optical order-disorder transition controlled by an intensive parameter come, to our knowledge, from the system based on a liquid-crystal light valve with 2D nonlocal feedback [8,10,23]. However, quantitative details of that transition have not yet been provided and the question is open whether an optical nonlinearity plus nonlocality can give rise to space-time chaotic states [23].

In this paper we report the quantitative characterization of

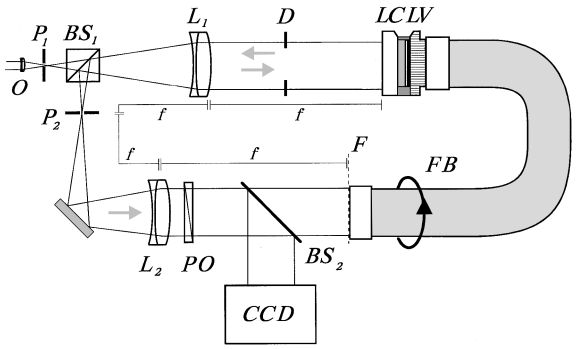

FIG. 1. Experimental setup. O=microscope objective; P_1,P_2=pinholes; BS_1, BS_2=beam splitters; LCLV=liquid-crystal light valve; L_1,L_2=lenses of f=25 cm focal length; D=diaphragm; FB=fiber bundle; CCD=videocamera. The $4f$ configuration of the feedback loop provides a 1 to 1 imaging of the front plane of the LCLV on the F plane.

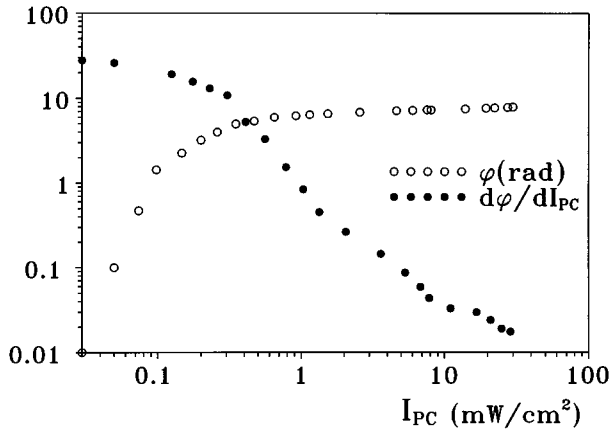

FIG. 2. Open loop phase shift induced by the writing intensity on the component of the reading light polarized along the liquid-crystal director.

a transition from ordered patterns to a space-time chaotic regime in a nonlinear optical system, by keeping a fixed Fresnel number and varying the level of excitation in the nonlinear medium. The experimental system consists of the same kind of nonlinear interferometer introduced in [8] and discussed in [10,23,24], in which the instabilities arise from the interplay between optical nonlinearity, excitation diffusion, and nonlocal interactions. These last ones are introduced via a rotation of the optical beam around its propagation axis. The spatial bandwidth of the excited signal is measured and compared with the theoretical predictions, leading to a discussion on the capability and limitations of the present experimental system.

II. TRANSITION FROM ORDERED PATTERNS TO SPACE-TIME CHAOS

The experimental setup is shown in Fig. 1. A light beam from an Ar^+ laser operating at a wavelength of 514 nm is expanded and filtered by means of the telescopic system formed by microscope objective O, pinhole P_1, and lens L_1. This beam is then sent on an optically addressable liquid-crystal light valve (LCLV) operating in reflection. This device utilizes the fact that nematic liquid-crystal (LC) molecules are strongly birefringent, in order to modulate the phase of the reflected light (''reading'' light) in the presence of another beam impinging on the rear side of the valve (''writing'' light). In fact, the birefringence of the liquid crystals is due to the average alignment of the anisotropic LC molecules along a preferential axis, called the LC director. By applying an ac voltage to a thin liquid-crystal layer, it is possible to induce a reorientation of the molecules, and hence to control the amount of birefringence of the layer.

In the LCLV, the mirror that reflects the reading light is sandwiched between a LC layer in front of it, and a photoconductive layer behind it. By means of transparent electrodes an ac voltage is applied to the device. The fraction of voltage dropping across the LC layer depends on the local illumination on the photoconductor, and hence the intensity of the writing light determines the phase modulation on the reflected reading beam.

In our experiment, the light reflected by the LCLV is passed through the polarizer PO and imaged by means of lens L_2 on the plane F. By appropriately choosing the experimental geometry (see Fig. 1) we obtain on plane F a 1 to 1 image of the front plane of the LCLV. This image is then fed back on the rear side of the valve by means of the fiber bundle FB. The use of the fiber bundle allows to rotate the feedback image by an angle Δ, thus establishing a nonlocal interaction of the material excitation with itself. The videocamera charge-coupled-device allows visualization and acquisition of the image on the F plane. We stress that in the present geometry, that is, with the use of an image forming feedback path, diffraction plays no role at all in the experiment, at variance with the situation already investigated using a similar setup [15,16].

Since the LCLV acts on the phase of the reading beam, but it is sensitive to the intensity of the writing beam, an effective feedback requires conversion of phase into intensity modulation. This is provided by the polarizer PO in the feedback loop. In our experiment the input light is vertically polarized, the LC director forms an angle of 45° with the vertical direction, and the polarizer nontransmissive axis is horizontal. In these conditions the light intensity reaching the photoconductor on the rear plane of the LCLV has the expression

$$I_{\mathrm{pc}}=R\left\{\frac{rI_0}{2}\left[1+\cos\varphi\right]\right\}, \tag{1}$$

where R represents the operator introduced by means of the fiber bundle rotation, r=0.21 is an overall reflection factor, I_0 is the input intensity, and $\varphi=u(I_{\mathrm{pc}})+\varphi_0(V_0)$ is the phase shift induced by the LCLV on the component of the input light parallel to the LC director. This phase shift is the sum of a part $\varphi_0(V_0)$ that exists always in presence of the applied voltage V_0, plus an additional part $u(I_{\mathrm{pc}})$ due to the presence of the writing light.

In our experiment we keep fixed the input intensity I_0=9.5 mW/cm^2, the feedback rotation angle Δ=30°, the 10-mm diam. of the diaphragm D in front of the LCLV, and use the voltage applied to the LCLV as a control parameter. Though V_0 is an intrinsic parameter, it is in principle possible that, since a variation of V_0 induces a variation in the sensi-

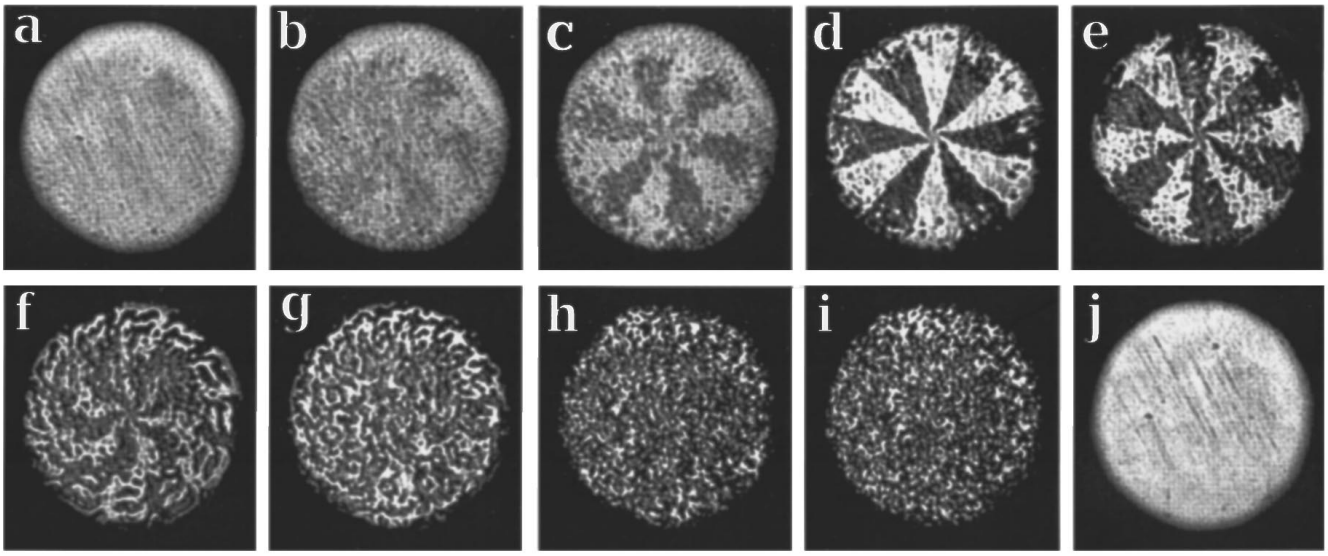

FIG. 3. Patterns observed on the rear side of the LCLV for increasing values of the voltage V_0 (Vrms). (a) $V_0=12.0$, (b) $V_0=12.4$, (c) $V_0=12.8$, (d) $V_0=13.2$, (e) $V_0=13.6$, (f) $V_0=13.8$, (g) $V_0=14.0$, (h) $V_0=14.4$, (i) $V_0=14.8$, (j) $V_0=15.2$.

tivity of the optical nonlinearity, it results in a variation of the area over which the input intensity is above the pattern formation threshold. This is due to the Gaussian profile of the input wave, and can result in a variation of the effective Fresnel number of the system, as discussed in [25]. Since the input wave in our case is a Gaussian beam that expands to a radius of $\simeq$15 mm half width at half maximum, and the radius of the aperture limiting the system is 5 mm, we expect indeed that this effect is not strong in the present experimental conditions.

The supply voltage applied to the LCLV is a sinusoidal wave at a fixed frequency of 2 kHz, and with a rms amplitude that varies between 12 and 15.5 V. In this range, the stationary open loop response of the LCLV to writing intensity $u(I_{pc})$ is with a good approximation independent of V_0. The modulus of this function is reported in Fig. 2 together with its derivative. Indeed, since the LCLV nonlinearity is of defocusing type, the sign of $u(I_{pc})$ is always negative. From Fig. 2 it results that the response of the LCLV is linear in the writing intensity (Kerr-like) only for a limited range of intensities.

In Fig. 3 we show the sequence of patterns observed when varying V_0 between 12 and 15.2 V. The space-time evolution of these patterns has also been visualized, by digitizing the signal on a circle with a diameter of 9 mm at time intervals of 1 sec. The digitization of each time series has started $\simeq$1 min after adjusting the value of V_0, in order to avoid possible transient effects. The resulting space-time plots are shown in Fig. 4. For $V_0\leqslant$12.5 V the output pattern is stationary and homogeneous, apart from a noise distribution that is present on the LCLV [Figs. 3(a) and 4(a)]. Then a six petal structure begins to appear, reaching its maximum visibility around $V_0=13.5$ V. [Figs. 3(c)–3(e)]. This structure is stationary [Fig. 4(b)], in agreement with what was reported in [23].

When the voltage is still increased ($V_0\simeq$13.8 V), the six petal structure begins to break, sometimes showing a sort of spatial period doubling [Figs. 3(f) and 4(c)] and temporal fluctuations. For V_0 between 14 and 14.8 V the regular pattern disappears completely, and a space-time chaotic situation is reached [Figs. 3(g)–3(i), 4(d), and 4(e)]. Finally, at $V_0=15.2$ V an abrupt transition is observed from the space-time chaotic regime to an homogeneous and stationary pattern, similar to that observed at $V_0=12.0$ V [Figs. 3(j) and 4(f)].

A first quantitative characterization of the observed transition is provided by the second-order intensity structure function, defined as

$$S(\theta)=\frac{\langle[I(r_0,\theta_0,t)-I(r_0,\theta_0+\theta,t)]^2\rangle}{2\langle I^2(r_0,\theta_0,t)\rangle}. \qquad (2)$$

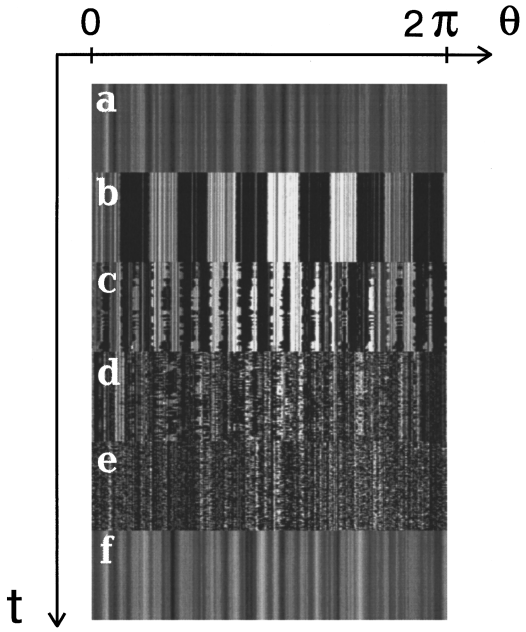

FIG. 4. Space-time evolution of the signal on a circle of diameter $D=9$ mm for increasing values of the voltage V_0 (Vrms). (a) $V_0=12.0$, (b) $V_0=13.4$, (c) $V_0=13.9$, (d) $V_0=14.3$, (e) $V_0=14.8$, (f) $V_0=15.2$. For any value of V_0 the signal is displayed for 128 sec.

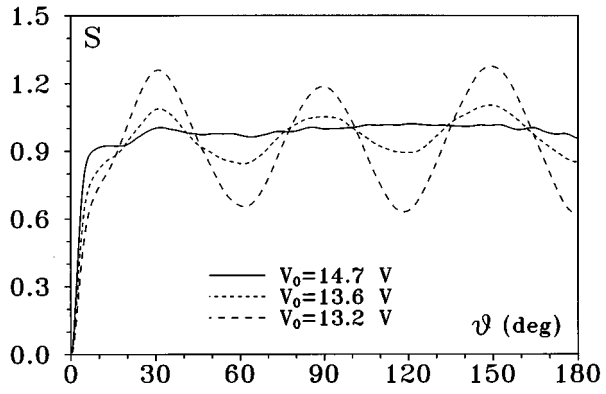

FIG. 5. Second-order structure function of the signal measured on a circle of diameter $D=9$ mm.

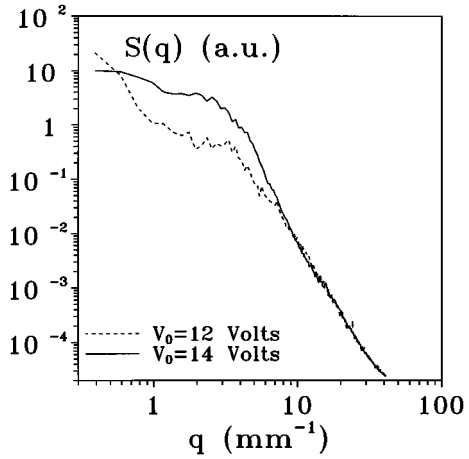

FIG. 6. Power spectra of the signal (see text for the definition) for $V_0=12.0$ (dashed line) and for $V_0=14.0$ V (solid line). The curve for $V_0=12$ V is the noise spectrum.

We fix $r_0=4.5$ mm, corresponding to the same radius at which Fig. 4 was recorded. Here $\langle\ \rangle$ denotes a double average, first on time and then on the azimuthal coordinate θ_0. The structure function is reported in Fig. 5 for three different values of V_0. It can be seen that the pattern is fully correlated in the six petal regime ($V_0=13.2$ V), and it still has a long-range correlation when the structures begin to break ($V_0=13.6$ V). Finally, in the space-time chaotic regime ($V_0=14.7$ V) the dip of the structure function close to $\theta=0$ is very narrow, indicating that the system is behaving like a set of uncorrelated domains.

In order to give an indicator of the degree of complexity that is present in the disordered state, beside the structure function, we can evaluate the bandwidth of the excited modes. If we associated a mode with a spatial Fourier component q, the bandwidth $\delta\tilde{q}$ of the spatial power spectrum gives directly this information.

We have measured the excited bandwidth for various values of V_0 using the following method. For any value of V_0 of our interest we have digitized a set of 20 patterns separated in time by 2 sec, and calculated the time-averaged spatial power spectrum of these signals. The two-dimensional spectra obtained in this way have been reduced to one-dimensional spectra by integrating over shells of constant radius in the Fourier plane. These one-dimensional spectra are then compared with the noise spectrum measured at $V_0=12$ V, i.e., when the system is in the homogeneous uniform state. This noise spectrum is shown in Fig. 6 together with the pattern spectrum for $V_0=14$ V. From the comparison of the two curves, it is possible to determine the largest excited wave number as the highest $\tilde{q}$ value beyond which the signal spectrum merges with the noise spectrum. It can be seen that the maximum spatial frequency excited in the system results in being around 10 mm^{-1}. Since the optical aperture limiting the system has a 10-mm diam it follows that for $V_0\simeq 14.5$ V the signal behaves as a collection of some hundreds of uncorrelated domains. With these conditions we are therefore in the presence of a well developed space-time chaotic regime.

We remark that, even if the whole set of experiments reported here is carried out for $\Delta=30°$, qualitative identical results have been obtained for any value not too small of Δ of the form $\Delta=(2\pi/N)$, with N an even integer. It is worth also noting that, since a variation of V_0 corresponds to a change in the sensitivity of the optical nonlinearity, it is to be expected that a scenario similar to that reported here by varying V_0 be observable if V_0 is kept fixed, and the input intensity I_0 is used as a control parameter. This conjecture has been confirmed by the experiments.

III. EVALUATION OF THE MARGINAL STABILITY CURVE AND COMPARISON WITH THE EXPERIMENT

Theoretical and numerical analyses of the experimental system under consideration have been given in [23,26,27], starting from the equation for the evolution of the phase shift u:

$$\frac{\partial u(\vec{r},t)}{\partial t}=-\frac{u(\vec{r},t)}{\tau}+D\nabla^2 u(\vec{r},t)+R\{\gamma I_0(1+\cos[u(\vec{r},t)+\varphi_0])\},\qquad(3)$$

where R denotes the rotation operator, the constant γ is comprehensive of both the optical losses of the feedback loop and the responsivity of the LCLV, τ is the response time, and D is the diffusion constant of the LCLV. The source term is proportional to the feedback intensity I_{pc} on the photoconductor, given by Eq. (1).

In the absence of the rotation operator, Eq. (3) gives rise to optical bistability for sufficiently high values of γI_0. It has been shown [23] that the introduction of the rotation can lead to the destabilization of the spatially uniform solutions, giving rise to transverse pattern formation. This occurs via the excitation of a band of transverse wave vectors $\vec{q}$ symmetrically arranged around the origin in the Fourier plane.

In the conditions of our experiments, the light intensity I_{pc} on the photoconductor varies approximately between 0 and 2 mW/cm^2. As shown in Fig. 2, in this range the response of the LCLV is strongly nonlinear in intensity. However, using very small input intensities, that is, using only the linear part of the LCLV characteristic, we do not reproduce the observed phenomena, because no bifurcation occurs from the uniform state. Indeed in this last case the level of excitation of the liquid crystal is too small. Due to these considerations,

it is clearly unrealistic to expect a good quantitative agreement between the experiment and the model of Eq. (3), which implies a linear response of the LCLV to the writing intensity. We therefore introduce a modified version of Eq. (3) of the form

$$\frac{\partial u(\vec{r},t)}{\partial t} = -\frac{u(\vec{r},t)}{\tau} + D\nabla^2 u(\vec{r},t) - \gamma R\{f[I_{\rm pc}(\vec{r},t)]\}, \quad (4)$$

where the minus sign for the source term is reminiscent of the fact that the medium is defocusing, and the function $f(I_{\rm pc})$ describes the nonlinear response of the LCLV to the writing intensity. The equilibrium solution of Eq. (4) in the absence of rotation

$$\bar{u} = -\gamma\tau f(I_{\rm pc}) \quad (5)$$

is just the open loop response of the LCLV, the modulus of which is plotted in Fig. 2. Substituting expression (1) for the feedback intensity into Eq. (4), we obtain

$$\tau\frac{\partial u}{\partial t} = -u + l_d^2\nabla^2 u - \gamma\tau R\left\{ f\left(\frac{rI_0}{2}\{1+\cos[u+\varphi_0(V_0)]\}\right)\right\}, \quad (6)$$

where the diffusion length $l_d = \sqrt{D\tau}$ has been introduced. Equation (6) admits the homogeneous stationary solution:

$$\tilde{u} = -\gamma\tau f\left(\frac{rI_0}{2}\{1+\cos[\tilde{u}+\varphi_0(V_0)]\}\right) \equiv -\gamma\tau f(I_{\rm pc}[\tilde{u}+\varphi_0(V_0)]). \quad (7)$$

We stress that Eqs. (5) and (7) have a different meaning. In fact, while Eq. (5) refers to an open loop situation, Eq. (7) takes into account the particular kind of feedback that we have imposed. For the values of the parameters used in our experiments, Eq. (7) implies a bistability for the phase $\tilde{u}$. Let us now add a perturbation to the homogeneous stationary solution (7),

$$u(\vec{r},t) = \tilde{u} + \xi(\vec{r},t). \quad (8)$$

Substituting into Eq. (6) and linearizing gives

$$\tau\frac{\partial\xi}{\partial t} = -\xi + l_d^2\nabla^2\xi + \Gamma R\xi, \quad (9)$$

where the coupling constant Γ is

$$\Gamma = \gamma\tau\frac{rI_0}{2}\left.\frac{\partial f}{\partial I_{\rm pc}}\right|_{I_{\rm pc}[\tilde{u}+\varphi_0(V_0)]}\sin[\tilde{u}+\varphi_0(V_0)]. \quad (10)$$

For I_0 fixed, Γ depends only on V_0.

It is possible to evaluate experimentally the behavior of the function $\Gamma(V_0)$. In order to do this, we must know the behavior of the derivative $\gamma\tau(df/dI_{\rm pc})$, that is easily obtainable from Fig. 2 with the use of Eq. (5). Furthermore, we need to know the functional shape of $I_{\rm pc}[\tilde{u}+\varphi_0(V_0)]$. This task is accomplished by measuring the intensity $I_{\rm pc}$ on the photoconductor at closed loop vs V_0, in the absence of rotation. The result of this measurement, done by extracting a fraction of the feedback light via the beam splitter BS_2 in Fig. 1, is shown in Fig. 7. The bistable behavior of the device is clearly visible near $V_0 = 15$ V rms. However, the presence of small spatial inhomogeneities on the LCLV surface ("noise") prevents from observing an hysteresis cycle. Figure 7 also clarifies the nature of the abrupt transition from the space-time chaotic regime to the homogeneous stationary solution that is observed when increasing V_0 from 14.8 to 15.2 V. This transition is due to the jump of the system to a new fixed point, the solution of the bistability equation.

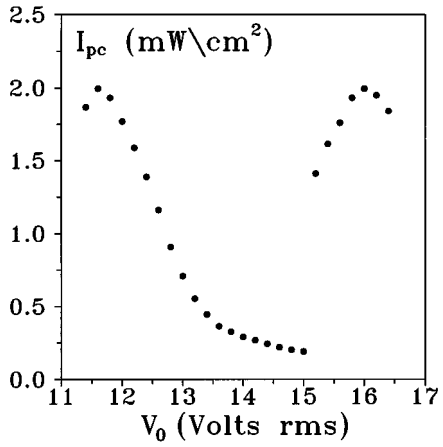

FIG. 7. Closed loop intensity on the photoconductor vs applied voltage, in the absence of rotation in the feedback loop. Bistability of the system is manifested with the jump in intensity observed at $V_0 \simeq 15$ V.

By using Eq. (1) and relating the feedback intensity $I_{\rm pc}$ to the phase $\tilde{u}+\varphi_0(V_0)$, it is possible to extract the value of this phase from the intensity measurement shown in Fig. 7. It is then possible to combine together all these elements in the relation (10) for $\Gamma(V_0)$. The modulus of Γ vs V_0 is reported in

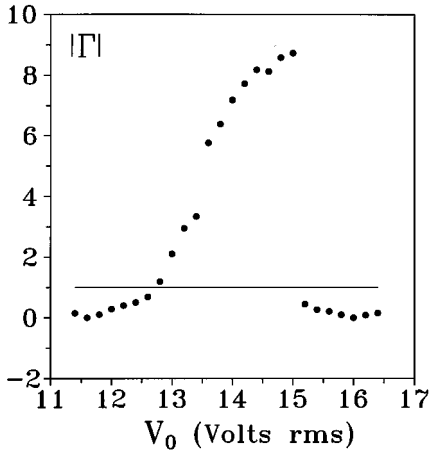

FIG. 8. Modulus of the coupling constant Γ [see Eq. (10)] vs the applied voltage. Homogeneous perturbations are damped for $|\Gamma|<1$, amplified for $|\Gamma|>1$.

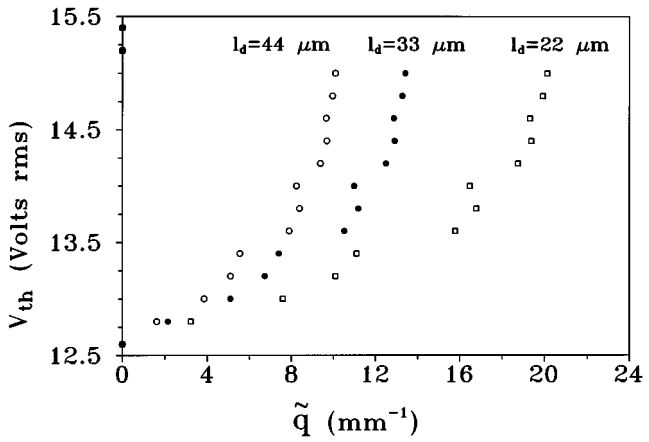

FIG. 9. Marginal stability curve in the $\tilde{q}$-$V_{0_{th}}$ plane; $\tilde{q}=1/\Lambda$, Λ being the wavelength of the perturbation considered.

Fig. 8. As we shall see, this is the relevant quantity with respect to the dynamics of the system.

Coming back to Eq. (9), if we want to evaluate the bandwidth of the excited modes in the disordered regime, a question arises about the choice of the most convenient basis for expanding the perturbation ξ. Usually, the most appropriate approach for the description of the patterned state is the expansion in a series of Bessel functions [23,27] because these functions are close to the shape of the observed patterns, since they are the solution of the diffraction problem. However, if we are not interested in the low-dimensional regime, in which there is an interplay between only a few modes, but we want to evaluate the width of the marginal stability curve in the high-dimensional regime, it seems more appropriate to use a Fourier expansion. This approach does not retain the structural features of the patterns, but gives a description in terms of the band of spatial frequencies excited, which we want to use as an indicator of the degree of complexity of the disordered state. The Fourier expansion was originally applied to the study of the present problem in Ref. [26]. In our analysis we will follow closely that approach, but we introduce furthermore the specific shape of our LCLV characteristics in order to be able to compare the theoretical predictions with the results of the experiment.

If we limit ourselves to considering the case of a rotation in the feedback of an angle $\Delta=(2\pi/N)$ with N integer, we can, following Ref. [26], expand the perturbation $\xi(\vec{r},t)$ onto a finite basis of N plane waves:

$$\xi(\vec{r},t)=\sum_{j=1}^{N} a_j(t)\cos(\vec{K}_j\cdot\vec{r}), \tag{11}$$

where $\vec{K}_j=(q,j\Delta)$ for $j=1,\ldots,N$ is the jth wave vector expressed in polar coordinates in the Fourier plane. In other words, we choose for the perturbation field a basis formed by N wave vectors of equal wave number q, and rotated of an angle Δ, each one with respect to the following. We adopt this choice that led to a fair agreement between theoretical analysis and numerical simulations in [19].

From the definition of the basis vectors $\vec{K}_j$ it follows that the effect of the rotation operator R on each component of the perturbation is

$$R\{a_j(t)\cos(\vec{K}_j\cdot\vec{r})\}=a_j(t)\cos(\vec{K}_{j+1}\cdot\vec{r}), \tag{12}$$

so that, by substitution of the expression (11) in the linearized equation (9), we obtain

$$\tau\frac{d}{dt}\begin{pmatrix} a_1\\ a_2\\ a_3\\ a_4\\ \vdots\\ a_N\end{pmatrix}=\begin{pmatrix} \alpha & 0 & 0 & \cdots & 0 & \Gamma\\ \Gamma & \alpha & 0 & \cdots & 0 & 0\\ 0 & \Gamma & \alpha & \cdots & 0 & 0\\ \vdots & \vdots & \vdots & \ddots & \vdots & \vdots\\ 0 & 0 & 0 & \cdots & \alpha & 0\\ 0 & 0 & 0 & \cdots & \Gamma & \alpha\end{pmatrix}\begin{pmatrix} a_1\\ a_2\\ a_3\\ a_4\\ \vdots\\ a_N\end{pmatrix}$$

$$\equiv M\begin{pmatrix} a_1\\ a_2\\ a_3\\ a_4\\ \vdots\\ a_N\end{pmatrix}, \tag{13}$$

where $\alpha\equiv-1-l_d^2q^2$. In our experiments, $\Delta=30°=2\pi/N$ with $N=12$, so that we are interested at the eigenvalues of the matrix M for N even. In this case, the following two real eigenvalues exist:

$$\lambda_{\pm}=-1-l_d^2q^2\pm\Gamma, \tag{14}$$

hence, whatever the sign of Γ, the eigenvalue with maximal real part is

$$\bar{\lambda}=-1-l_d^2q^2+|\Gamma|. \tag{15}$$

This eigenvalue determines the stability of the homogeneous stationary solution. As previously stated, it depends only on the modulus of Γ and not on its sign. The fact that the first unstable eigenvalue is purely real is in agreement with the stationary nature of the pattern observed just above threshold.

Having measured the dependence of $|\Gamma|$ vs V_0, Eq. (15) permits us to draw the marginal stability curve in the $\tilde{q}$-V_0 plane (we define here $\tilde{q}=q/2\pi$); that is, the locus of points satisfying the threshold condition

$$|\Gamma(V_{0_{th}})|-1-4\pi^2l_d^2\tilde{q}^2=0. \tag{16}$$

Three of these curves are plotted in Fig. 9 for different values of the diffusion length l_D. It is worth noting that, though it is known that l_d is of the order of the tens of microns, its precise value depends on the specific experimental conditions (e.g., level of illumination, applied voltage).

From Eq. (16) we obtain that the excited band depends on V_0 as

$$\Delta\tilde{q}\equiv\frac{1}{\Lambda_{\min}}=\frac{\sqrt{|\Gamma(V_0)|-1}}{2\pi l_d}, \tag{17}$$

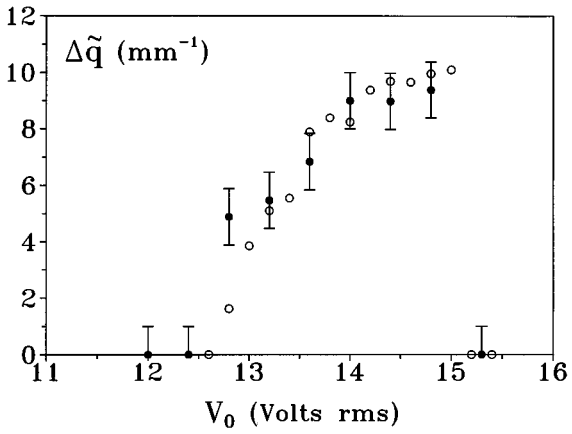

FIG. 10. Excited bandwidth $\Delta\tilde{q}$ vs applied voltage V_0. Filled dots, experimental spectral widths; empty dots, predictions obtained by solving Eq. (17) and using the data shown in Fig. 8.

where $\Lambda_{\min}$ is the shortest wavelength excited in the pattern. A direct comparison with the experimental data is shown in Fig. 10, where the values of $\Delta\tilde{q}$vsV_0 measured using the procedure described in Sec. III are reported together with their counterpart, calculated using Eq. (17). A good agreement between model and experiment is obtained for l_D=44 μm.

IV. CONCLUSIONS

We have experimentally investigated the dynamical behavior of a nonlinear optical system based on a liquid-crystal light valve when a nonlocal interaction is introduced. A transition from a uniform state to a patterned state and eventually to space-time chaos state, has been shown by varying an intensive parameter.

The theoretical analysis gives results in good agreement with the experiments, provided the nonlinear in intensity response of the LCLV is taken into account. From the analysis it results also that there is an intrinsic limitation to the level of ''useful'' excitation at which the system can be brought, and hence to the highest spatial frequency that can be destabilized. This limitation comes from the fact that the system, even in presence of rotation in the feedback, is reminiscent of the homogeneous stationary states given by the bistability equation governing it in the absence of rotation. Thus, for high levels of excitation, the system jumps to a new homogeneous stationary state (from which it can start a new cycle of transitions) rather than becoming more and more chaotic.

However, in the most disordered state the measured structure functions and power spectra show a sharp decay that is a characteristic feature of space-time chaos, while there is no evidence of a power-law behavior. Therefore we cannot strictly speak of a turbulent regime, since there is no signature of the self-similarity properties of turbulence.

ACKNOWLEDGMENTS

We acknowledge A. Consortini for fruitful discussions. This work has been partially supported by the EEC contribution for the Joint Research Project on Spatio-Temporal Dynamics in Lasers (Contract No. CI1*-CT93-0331).

[1] See, for example, M. C. Cross and P. C. Hohenberg, Rev. Mod. Phys. **65**, 851 (1993).
[2] J. D. Murray, *Mathematical Biology* (Springer-Verlag, Berlin, 1989).
[3] See, e.g., *Nonlinear Dynamics and Spatial Complexity in Optical Systems*, edited by R. G. Harrison and J. S. Uppal (SUSSP Publications, Edinburgh, and Institute of Physics Publishing, London, 1993).
[4] A. G. Fox and T. Li, Bell Syst. Tech. J. **40**, 453 (1961).
[5] F. T. Arecchi, G. Giacomelli, P. L. Ramazza, and S. Residori, Phys. Rev. Lett. **65**, 2531 (1990).
[6] E. J. D'Angelo, E. Izaguirre, G. B. Mindlin, G. Huyet, L. Gil, and J. R. Tredicce, Phys. Rev. Lett. **68**, 3702 (1992); F. T. Arecchi, S. Boccaletti, G. B. Mindlin, and C. Perez Garcia, *ibid*. **69**, 3723 (1992); J. Y. Courtois and G. Grynberg, Opt. Commun. **87**, 186 (1992).
[7] M. Brambilla, M. Cattaneo, L. A. Lugiato, R. Pirovano, F. Prati, A. J. Kent, G. L. Oppo, A. B. Coates, C. O. Weiss, C. Green, E. J. D'Angelo, and J. R. Tredicce, Phys. Rev. A **49**, 1427 (1994), and references therein.
[8] S. A. Akhmanov, M. A. Vorontsov, and V. Yu. Ivanov, Pis'ma Zh. Eksp. Teor. Fiz. **47**, 611 (1988) [JETP Lett. **47**, 707 (1988)].
[9] W. J. Firth, J. Mod. Opt. **37**, 151 (1990); G. D'Alessandro and W. J. Firth, Phys. Rev. Lett. **66**, 2597 (1991).
[10] M. A. Vorontsov, SPIE Proc. **1402**, 116 (1990).
[11] R. Macdonald and H. J. Eichler, Opt. Commun. **89**, 289 (1992); M. Tamburrini, M. Bonavita, S. Wabnitz, and E. Santamato, Opt. Lett. **18**, 855 (1993).
[12] F. Papoff, G. D'Alessandro, G. L. Oppo, and W. J. Firth, Phys. Rev. A **48**, 634 (1993).
[13] F. T. Arecchi, A. V. Larichev, and M. A. Vorontsov, Opt. Commun. **105**, 297 (1994); E. Pampaloni, P. L. Ramazza, S. Residori, and F. T. Arecchi, Europhys. Lett. **25**, 587 (1994).
[14] M. A. Vorontsov, Quantum Electron. **23**, 269 (1993).
[15] E. Pampaloni, S. Residori, and F. T. Arecchi, Europhys. Lett. **24**, 647 (1993).
[16] E. Pampaloni, P. L. Ramazza, S. Residori, and F. T. Arecchi, Phys. Rev. Lett. **74**, 258 (1995).
[17] F. T. Arecchi, G. Giacomelli, P. L. Ramazza, and S. Residori, Phys. Rev. Lett. **67**, 3749 (1991); G. Indebetouw and S. Liu, Opt. Commun. **91**, 321 (1992).
[18] D. Dangoisse, D. Hennequin, C. Lepers, E. Lovergnaux, and P. Glorieux, Phys. Rev. A **46**, 5955 (1992).
[19] M. Kreuzer, W. Balzer, and T. Tschudi, Appl. Opt. **29**, 579 (1990); R. Neubecker, M. Kreuzer, and T. Tschudi, Opt. Commun. **96**, 117 (1993).
[20] P. C. Hohenbeerg and B. I. Shraiman, Physica D **37**, 109 (1989).
[21] F. T. Arecchi, S. Boccaletti, P. L. Ramazza, and S. Residori,

Phys. Rev. Lett. **70**, 2277 (1993).
[22] J. V. Moloney, P. K. Jacobsen, J. Lega, S. G. Wenden, and A. C. Newell, Physica D **68**, 127 (1993).
[23] S. A. Akhmanov, M. A. Vorontsov, and V. Yu. Ivanov, A. V. Larichev, and N. I. Zheleznykh, J. Opt. Soc. Am. B **9**, 78 (1992).
[24] F. T. Arecchi, A. Larichev, P. L. Ramazza, S. Residori, J. C. Ricklin, and M. A. Vorontsov, Opt. Commun. **117**, 492 (1995).
[25] R. Macdonald and H. Danlewski, Opt. Commun. **113**, 111 (1994); R. Macdonald and H. Danlewski, Opt. Lett. **20**, 441 (1995).
[26] H. Adachihara and H. Faid, J. Opt. Soc. Am. B **10**, 1242 (1993).
[27] N. I. Zheleznykh, M. Le Berre, E. Ressayre, and A. Tallet, *Nonlinear Optical Structures, Patterns, Chaos*, edited by L. A. Lugiato, special issue of Chaos, Solitons and Fractals **4**, 1717 (1994); M. A. Vorontsov and W. J. Firth, Phys. Rev. A **49**, 2891 (1994).